ORIGINAL RESEARCH

Cytotoxicity of nickel zinc ferrite nanoparticles on cancer cells of epithelial origin

Mothanna Sadiq Al-Qubaisi[1]
Abdullah Rasedee[1,2]
Moayad Husein Flaifel[5]
Sahrim HJ Ahmad[5]
Samer Hussein-Al-Ali[1]
Mohd Zobir Hussein[3]
Eltayeb EM Eid[6]
Zulkarnain Zainal[3]
Mohd Saeed[1]
Muna Ilowefah[4]
Sharida Fakurazi[1]
Norhaszalina Mohd Isa[1]
Mohamed Ezzat El Zowalaty[1,7]

[1]Institute of Bioscience, [2]Faculty of Veterinary Medicine, [3]Department of Chemistry, Faculty of Science, [4]Faculty of Food Science and Technology, Universiti Putra Malaysia, Selangor, Malaysia; [5]School of Applied Physics, Faculty of Science and Technology, Universiti Kebangsaan Malaysia, Selangor, Malaysia; [6]College of Pharmacy, Qassim University, Buraidah, Saudi Arabia; [7]Faculty of Pharmacy, Zagazig University, Ash Sharqiyah, Egypt

Correspondence: Rasedee Abdullah
Faculty of Veterinary Medicine, Universiti Putra Malaysia, 43400 UPM Serdang, Selangor, Malaysia
Tel +603 8946 3455
Fax +603 8946 1971
Email rasedee@vet.upm.edu.my

Abstract: In this study, in vitro cytotoxicity of nickel zinc (NiZn) ferrite nanoparticles against human colon cancer HT29, breast cancer MCF7, and liver cancer HepG2 cells was examined. The morphology, homogeneity, and elemental composition of NiZn ferrite nanoparticles were investigated by scanning electron microscopy, transmission electron microscopy, and energy dispersive X-ray spectroscopy, respectively. The exposure of cancer cells to NiZn ferrite nanoparticles (15.6–1,000 µg/mL; 72 hours) has resulted in a dose-dependent inhibition of cell growth determined by MTT (3-(4,5-dimethylthiazol-2-yl)-2,5-diphenyltetrazolium bromide) assay. The quantification of caspase-3 and -9 activities and DNA fragmentation to assess the cell death pathway of the treated cells showed that both were stimulated when exposed to NiZn ferrite nanoparticles. Light microscopy examination of the cells exposed to NiZn ferrite nanoparticles demonstrated significant changes in cellular morphology. The HepG2 cells were most prone to apoptosis among the three cells lines examined, as the result of treatment with NiZn nanoparticles. In conclusion, NiZn ferrite nanoparticles are suggested to have potential cytotoxicity against cancer cells.

Keywords: NiZn ferrite nanoparticles, cancer cells lines, anticancer, apoptosis

Introduction

Magnetic nanoparticles are used in many biological and medical applications due to their interesting properties such as superparamagnetic behavior, high surface-to-volume ratio, and external magnetic force.[1] For instance, their high surface area and ability to bind with suspended antibiotic-resistant bacteria has encouraged environmental researchers to use them in the treatment of polluted waste water.[2]

Magnetic nanoparticles also represent a new era of promising applications in counteracting nosocomial infections, where microorganisms tend to attach and subsequently grow on solid surfaces, including medical devices, and form biofilms.[3] The presence of these microbial biofilms is a critical problem in the biomedical field. Microbial biofilms act as barriers against the action of antimicrobial agents, which become refractory to antimicrobial therapy. Different approaches have been applied to protect solid surfaces against colonization and biofilm formation, such as the use of nanoparticle-coated surfaces.[4]

In anticancer studies, magnetic nanoparticles are widely used in medical examinations, targeting, and treatment.[5] For detection purposes, incorporating magnetic nanoparticles into imaging modalities, such as magnetic resonance imaging (MRI), confers enhanced performance to cancer diagnosis.[6] In another advanced study, magnetic nanoparticles were utilized to detect tumors with diameters as small as 10 mm,

which enabled medical doctors to discover cancers at early stages of malignancy.[7] This diagnosis became known as the targeted-detection technique.[8,9]

Magnetic fluid hyperthermia is another medical application intended to inhibit tumor cell growth.[10] This application allows the insertion of magnetic nanoparticles into solid tumors followed by exposure to an alternating current (AC) magnetic field, which increases the temperature and subsequently kills the cancer cells with fewer side effects on normal cells.[11]

Magnetic nanoparticles are considered good carriers for many chemotherapeutic agents.[12,13] For example, in vivo injection of doxorubicin-loaded magnetic nanoparticles intratumorally into mice implanted subcutaneously with lung carcinoma has resulted in an increase in the efficacy of doxorubicin against tumors.[14]

HepG2, HT29, and MCF7 are three cell lines of epithelial origin that were isolated from the hepatocellular carcinoma of a 15-year-old male adolescent, the colorectal adenocarcinoma of a 44-year-old female adult, and the breast carcinoma of a 69-year-old female adult, respectively. MCF10a is a nontumorigenic epithelial cell line isolated from the mammary gland of a 36-year-old female adult (American Type Culture Collection [ATCC], Rockville, MD, USA).

Doxorubicin is one of the best drugs for systemic chemotherapy, which works against breast cancer. For colon cancer treatment, oxaliplatin is commonly used, while tamoxifen is the most common drug used for liver cancer. Most chemotherapies are expensive and cause serious side effects ranging from nausea, vomiting, mucositis, ulceration and necrosis of the colon to acute myeloid leukemia with a preleukemic phase and heart failure.[15]

Several reports clearly show that different types of magnetic nanoparticles are toxic to different types of cancer cells cultured in vitro including human SK-MEL-37 melanoma cells,[16] human osteosarcoma Saos-2 cells,[17] and cervical adenocarcinoma HeLa cells.[18] Current paradigms of apoptosis suggest that in mammalian cancer cells, the magnetic nanoparticles activate the oxidative stress by increasing reactive oxygen species (ROS) levels and depleting the antioxidant glutathione, which result in the induction of apoptosis via p53, survivin, bax/bcl-2, and caspase pathways.[19]

Very few studies have reported on the role of magnetic nanoparticles as anticancer materials. To our knowledge, this is the first report of the in vitro anticancer effect of nickel zinc (NiZn) ferrite nanoparticles against three cancer cell lines. The magnetic, structural, and morphological characteristics of NiZn ferrite nanoparticles were revealed. Further, the toxicity of NiZn ferrite nanoparticles against human colon cancer HT29, human breast cancer MCF7, and human liver cancer HepG2 cell lines was assessed and compared with the effects of oxaliplatin, doxorubicin, and tamoxifen, respectively. The mechanism of cytotoxicity of NiZn ferrite nanoparticles in these cancer cell lines is also discussed.

Methodology
Materials and preparation

Trypsin/ethylenediamine tetracetic acid (EDTA) solution was purchased from Invitrogen (Carlsbad, CA, USA). Dimethylsulfoxide (DMSO), phosphate-buffered saline (PBS), 3-(4,5-dimethylthiazol-2-yl)-2,5-diphenyltetrazolium bromide (MTT), Dulbecco's modified Eagle's medium (DMEM), diphenylamine (DPA) reagent (100 mL glacial acetic acid, 1.5 g diphenylamine, 1.5 mL concentrated sulfuric acid, 0.5 mL and 16 mg/mL acetaldehyde stock) and trypan blue dye were purchased from Sigma Chemical Company (Perth, WA, Australia). NiZn ferrite nanoparticle powder of the chemical formula $Ni_{0.5}Zn_{0.5}Fe_2O_4$ with 98.5% purity was procured from Nanostructured and Amorphous Materials Inc (Houston, TX, USA). The powder was formulated following techniques published previously.[20]

Characterization
Structure and morphology

Powder X-ray diffraction (XRD) patterns of NiZn ferrite nanoparticles were recorded with a Shimadzu XRD-6000 instrument (Shimadzu Corporation, Kyoto, Japan) in the range of 10°–70° using CuKα as a radiation source ($\lambda = 1.5418$ Å) generated at 30 kV and 30 mA. Fourier transform infrared (FTIR) spectra of NiZn ferrite nanoparticle powder were recorded over the range of 400–4000 cm^{-1} on a Thermo Nicolet Nexus, Smart Orbit spectrometer using a sample of approximately 1% in 200 mg of spectroscopic-grade potassium bromide (KBr) with 10 tons of pressure. Scanning electron microscopy (SEM, Model LEO 1450VP [LEO Electron Microscopy Ltd, Cambridge, UK]), with an accelerating voltage of 30 kV, and energy dispersive X-ray spectroscopy (EDX) were used in order to investigate the morphology and elemental composition of NiZn ferrite nanoparticles, respectively. In addition, transmission electron microscopy (TEM, Model CM12; Philips, Eindhoven, The Netherlands) with an accelerating voltage of 120 kV and a maximum magnification limit of 660 k times, was used to determine the homogeneity of the nanoparticles.

Cell culture

Three human cell lines were obtained from ATCC. The cell lines comprise human breast cancer (MCF7), human

colon cancer (HT29), human liver cancer (HepG2), and normal breast (MCF10a) cells, which are characterized as virus-negative. They grow as an adherent monolayer of tightly knit epithelial cells.

Cytotoxicity MTT assay

HT29, MCF7, and HepG2 cells lines were plated at 2×10^3 cells/well by adding 200 µL of a 1×10^4 cells/mL suspension to each well of a 96-well tissue culture plate. The plates were incubated for sufficient time to ensure attachment at 30% to 40% confluency. The media was aspirated off and replaced with fresh media (200 µL) containing NiZn ferrite of different concentrations (15.6 to 1,000 µg/mL) and chemotherapeutic agents at 0.156 to 10.0 µg/mL (oxaliplatin for HT29 cells, doxorubicin for both MCF7 and MCF10a cells, and tamoxifen for HepG2 cells). The last row was left as an untreated control. The plates were incubated at 37°C, 5% CO_2, for 72 hours. After incubation with the compounds, the media was aspirated off and the cells were washed by PBS buffer three times to ensure that all NiZn ferrite nanoparticles were removed, and then replaced with a fresh media. MTT solution (20 µL) in a total volume of 200 µL was added to every well and mixed gently with the media, which was later incubated for 4 to 6 hours at 37°C with 5% CO_2. The MTT-containing medium was then removed carefully and replaced with DMSO (200 µL per well) to dissolve the formazin crystals. The plates were read in a microtiter plate reader at 570 nm. The concentration of drug needed to inhibit cell growth by 50% (IC_{50}) was generated from the dose-response curves for each compound and each cell line.

Bromodeoxyuridine (BrdU) cell proliferation assay

To confirm antiproliferative effects in NiZn ferrite-treated cells, a BrdU cell proliferation kit was used. HepG2, MCF7, MCF10a, and HT29 cells were seeded at 1.5×10^5 cells/mL in a final volume of 100 µL in a 96-well culture dish and incubated overnight. The cells were treated with NiZn ferrite for 24, 48, and 72 hours, respectively. Then, BrdU label (20 µL, diluted by 1/2,000 in media) was added to each well and incubated for 24 hours at 37°C. The media was discarded and replaced by fix/denaturing solution (200 µL). The plate was incubated for 30 minutes at room temperature. The fix/denaturing solution was removed by inverting the plate. Then, BrdU antibody (100 µL, diluted by 1/100 in dilution buffer) was added to each well and left for 1 hour at room temperature. The cells were washed three times with wash buffer. After that, secondary antibody (100 µL, anti-mouse immunoglobulin G horseradish peroxidase-conjugated) was

added to each well for 30 minutes. The washing step was done three times with wash buffer and once with distilled water. The distilled water was removed and substrate solution (100 µL) was added to each well. The plate was left for 15 minutes at room temperature in the dark. Finally, a stop solution (100 µL) was added to the wells and absorbance measured at 450–540 nm.

Microscopic examination of cell morphology

HepG2, HT29, and MCF7 cells (1×10^4) were seeded in the 6-well plates and incubated overnight to allow the cells to adhere to the dish. The cells were exposed to NiZn ferrite nanoparticles for 72 hours at IC_{50} concentrations (calculated from MTT results). General morphology and membrane changes were examined via light-inverted microscope.

Caspase-3 and -9 assay

The extent of caspase-3 and -9 activation in HepG2, HT29, MCF10a, and MCF7 cells treated with 10, 50, 100, and 1000 µg/mL NiZn ferrite nanoparticle was assessed using a commercially available colorimetric assay kit in accordance with the protocol supplied by the manufacturer (Promega, Madison, WI, USA). The caspase activity in a sample is proportional to the amount of p-nitroaniline (pNA) product detected spectrophotometrically. This assay makes use of a caspase-specific substrate L-aspartic-L-glutamic-L-valyl-L-aspartic acid para-nitroaniline (DEVD-pNA) and L-leucine-L-glutamyl-L-histidyl-L-aspartic-p-nitroaniline acid amide (LEHD-pNA) labeled with pNA for caspase-3 and -9, respectively. Cleavage of the substrate by the specific cellular caspase yields free pNA that can be detected by spectrophotometer at 405 nm.

The cells were plated at a density of 1×10^6 cells/culture dish. After treatment with nanoparticles, the cells were harvested by centrifugation. The pellets were washed with PBS and lysed in 50 µL of chilled cell lyses buffer and left on ice for 10 minutes. The lysate was centrifuged at 50 g in Eppendorf Centrifuge 5810R (Hamburg, Germany) at 4°C for 5 minutes, and the supernatant was used for caspase assay. The caspase-3 and -9 activities were measured by the cleavage of colorimetric DEVD-pNA and LEHD-pNA. The production of pNA was estimated at 405 nm.

DNA fragmentation

DNA fragmentation was quantitatively determined using diphenylamine reagent. The cells were treated with NiZn ferrite nanoparticles at different concentrations, then harvested 12 and 24 hours after treatment. One hundred eight microliters of 5-molar perchloric acid was added to

the samples, which were then heated at 70°C for 15 minutes. Later, two volumes of a solution containing diphenylamine reagent were added, and then the samples were stored at 4°C for 48 hours. The colorimetric reaction was quantified at 575 nm using an ultraviolet-visible Thermo Smart Orbit spectrophotometer (Perkin Elmer, Waltham, MA, USA). DNA from both pellet and supernatant were quantified. The degree of DNA fragmentation is given by the following equation:

$$\text{Degree of DNA fragmentation} = (\text{DNA}_{\text{supernatant}}/\text{DNA}_{\text{(pellet + supernatant)}}) \times 100\% \quad (1)$$

Statistical analysis

All experiments were done at least three times unless otherwise indicated. Data are expressed as means ± standard deviation (SD). All statistical analyses were performed using Minitab statistical software (Minitab Inc, State College, PA, USA). Treatment effects were determined using one-way analysis of variance followed by Tukey's post hoc analysis. A value of $P < 0.05$ was considered significant unless indicated otherwise.

Results

XRD analysis

The XRD diffraction patterns of NiZn ferrite nanoparticles are depicted in Figure 1. In the studied angle range of $2\theta = 10°–70°$, it is clearly seen that the $Ni_{0.5}Zn_{0.5}Fe_2O_4$ powder has a crystalline phase with nine intense peaks which correspond to diffractions due to (111), (220), (311), (222), (400),
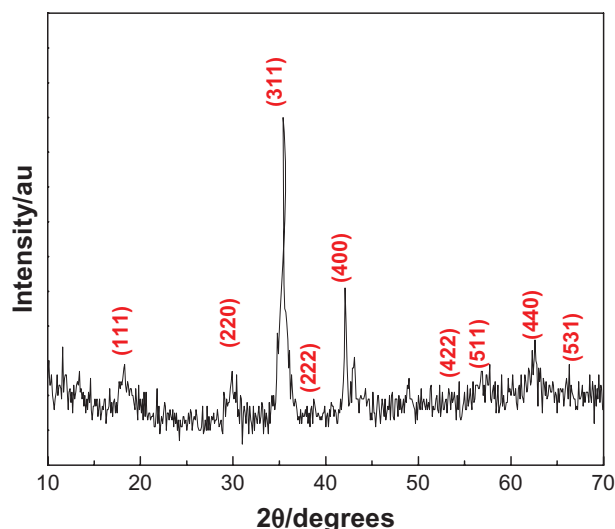
(422), (511), (440), and (531) planes. These planes are well indexed to a cubic spinel structure of a lattice parameter 8.4 Å with no impurity phase detected. The most intense peak of pure NiZn ferrite powder is assigned to the (311) index plane at $2\theta = 35.4°$. The particle size was calculated to be 12 nm using Debye–Scherrer's equation,

$$D = 0.9 \, \lambda/\beta\cos\theta, \quad (2)$$

where D is the crystallite size, λ is the incident X-ray wavelength, β is the full width at half-maximum, and θ is the diffraction angle.

Infrared spectroscopy

The FTIR spectrum for NiZn ferrite nanoparticles is shown in Figure 2. The spectrum was determined at a range of $400–4,000 \, cm^{-1}$ using a KBr pellet method. The strong absorption peak at $540 \, cm^{-1}$ is due to the characteristic stretching of NiZn ferrite nanoparticles. The absorption peaks at $3,344$ and $1,630 \, cm^{-1}$ for urea materials are attributed to stretching of the N—H (group NH_2) and C=O amide groups, respectively. These bands indicate that the urea may not be completely removed from the resulting material during the preparation process.

Morphological and elemental analysis of nanoparticles

The morphology of NiZn ferrite nanoparticles was examined with SEM. EDX was performed to confirm the elemental
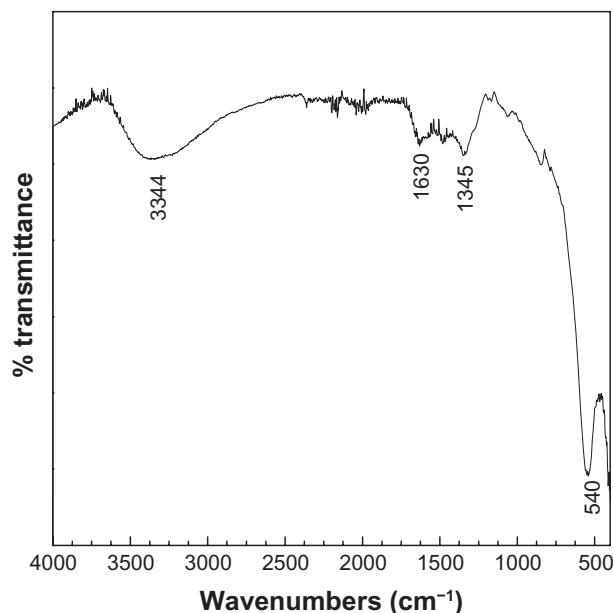

Figure 1 X-ray diffraction pattern of $Ni_{0.5}Zn_{0.5}Fe_2O_4$ powder.
Abbreviation: au, arbitrary unit.

Figure 2 Fourier transform infrared spectra of $Ni_{0.5}Zn_{0.5}Fe_2O_4$.
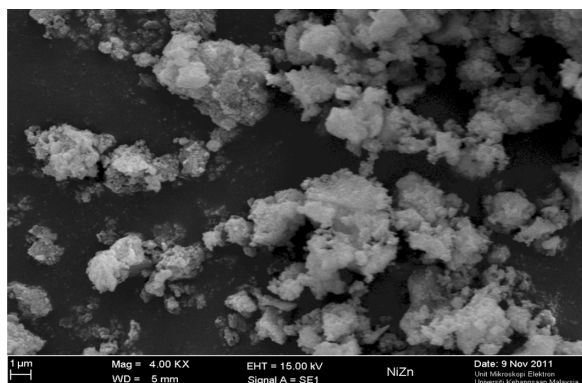
Figure 3 Scanning electron micrograph of pure NiZn ferrite nanoparticles.

composition of the pure sample. SEM and EDX micrographs for the pure sample are shown in Figures 3 and 4, respectively. It is clear that NiZn ferrite nanoparticles are agglomerated by forming bigger clusters, which is ascribed to their strong magnetic dipole–dipole interaction amongst the single-domain particles. It is believed that homogeneity could be enhanced, either by adding an appropriate agent or by using a proper homogenizing tool (eg, sonication, mechanical stirring, magnetic stirring etc), which would improve the overall physical properties of NiZn ferrite nanoparticles.

The morphology and the extent of dispersion of NiZn ferrite nanoparticles were determined with TEM. The TEM images of pure NiZn ferrite nanoparticles are shown in Figure 5. It is apparent that the nanoparticles are approximately spherical in shape with diameters ranging from 10 to 30 nm. In addition, most of the nanoparticles

are agglomerated, and few are detached. This behavior suggests the presence of high magnetic-dipole interparticle interactions among the NiZn ferrite nanoparticles.

Cellular sensitivity of cells to NiZn ferrite nanoparticles

The cytotoxicity of NiZn ferrite nanoparticles on the MCF7, HT29, and HepG2 cells was determined by MTT assay. Figure 6 shows that NiZn ferrite nanoparticles have significant cytotoxic effects against liver cancer HepG2 cells at all concentrations tested ($P < 0.05$). In the case of MCF7, the lowest concentration at 15.6 μg/L had no significant effect on cell growth, where the nanoparticles inhibited the growth of all cell lines tested in a dose-dependent manner.

The IC_{50} values of NiZn ferrite nanoparticles calculated from the dose-response curves are shown in Table 1. The results obtained from MTT assay showed significant change in the viability from HT29 cells treated with magnetic nanoparticles at concentrations of 31.3 and 62.5 μg/mL for 72 hours when compared to untreated cells. On the other hand, the normal breast MCF10a cells were the least sensitive to NiZn ferrite nanoparticles, with an IC_{50} value of approximately 915 μg/mL, while the breast cancer MCF7 cells were found to be more sensitive with an IC_{50} value of 58.7 μg/mL. The IC_{50} value of NiZn ferrite nanoparticles in normal breast MCF10 cells was almost 15 times higher than that in breast cancer MCF7 cells lines (Table 1). Furthermore, compared with NiZn ferrite nanoparticles, doxorubicin showed higher cytotoxicity in the normal breast MCF10a cell line.
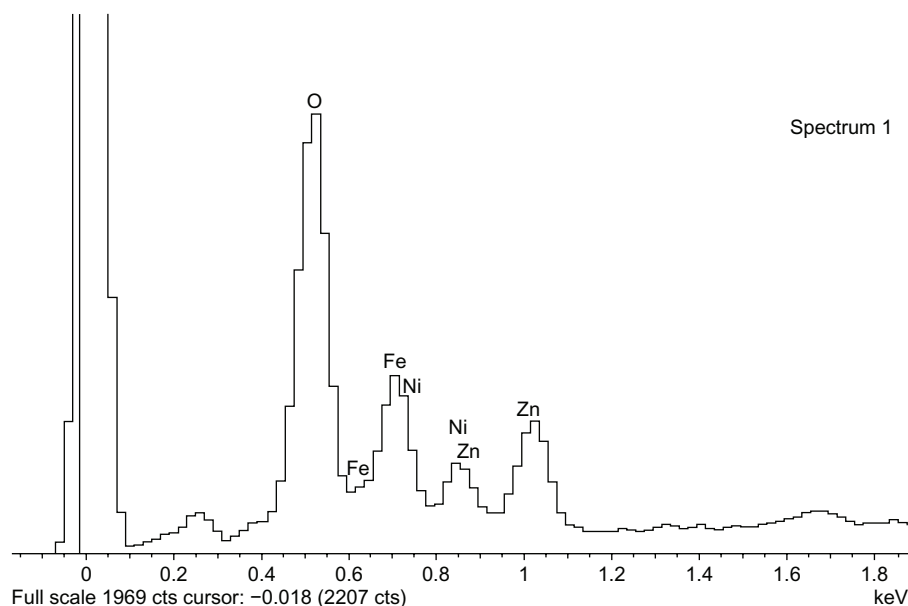

Figure 4 Energy dispersive X-ray spectroscopy of pure NiZn ferrite nanoparticles.
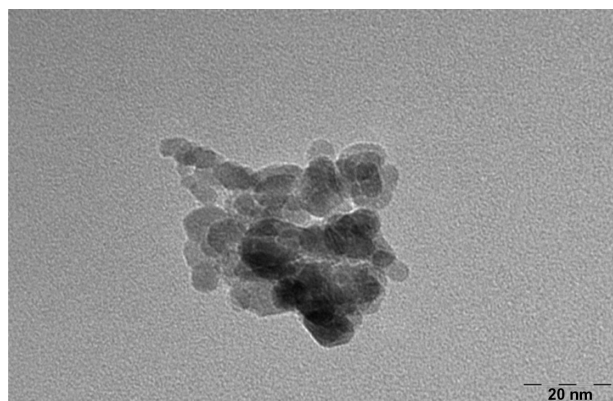**Abbreviations:** keV, kiloelectronvolt; Fe, iron; Ni, nickel; Zn, zinc; O, oxygen.

Figure 5 Transmission electron microscopy of pure NiZn ferrite nanoparticles.

Antiproliferative effect of NiZn ferrite nanoparticles

To evaluate the potential of NiZn ferrite nanoparticles in the inhibition of HepG2, HT29, and MCF7 cell proliferation, the cells were treated with various concentrations of the nanoparticles for 24, 48, and 72 hours. The effect of nanoparticles on the proliferation of the cultured cancer cells was measured by the incorporation of the thymidine analogue bromodeoxyuridine into DNA. The cell proliferation of the three cells lines decreased significantly after been treated with 100 µg/mL NiZn ferrite nanoparticles at 72 hours (Figure 7).

The antiproliferative effect of magnetic nanoparticles was evident on the HepG2 cells where 10 µg/mL NiZn ferrite nanoparticles decreased the optical density from 1.452 at 48 hours to 1.322 at 72 hours. Unlike HepG2, the proliferation of MCF7 cells incubated for 3 days was not affected by the same concentration of nanoparticles. On the other hand, the exposure of HT29 cells to 10 µg/mL NiZn ferrite nanoparticles for 24 and 72 hours resulted in a reduction in cell growth from 93% to 77% in comparison with the untreated cells (Figure 7). One hundred micrograms per milliliter exerted no significant growth inhibitory effects on MCF7 cells after 24 hours. At 1000 µg/mL, however, MCF10a proliferation appeared to be higher than that of the MCF7 cells.

Morphological examination of treated cells

The treatment for 72 hours at the respective IC_{50} concentrations of NiZn ferrite nanoparticles produced substantial morphological changes in HT29, MCF7, and HepG2 cells. The cells were detached, shrunken, and dispersed with membrane blebbing and cytoplasmic shrinkage (Figure 8).

However, these changes were more apparent in HepG2 cells than in the other two cancer cells lines (Figure 8).

Caspase-3 and -9

Caspase-9 is an initiator for the mitochondria-mediated (intrinsic) apoptotic pathway while caspase-3 is a major enzymatic marker of apoptosis. The caspase-3 and -9 activity of NiZn ferrite nanoparticle-treated cells was analyzed by CaspACE® colorimetric caspase assay kit (Promega). Figure 9 shows that activity of both caspases increased in HT29, MCF7 and HepG2 cells significantly as compared to untreated cells. In fact, the increase in caspase-3 and -9 activities seems to parallel the increase in NiZn ferrite nanoparticle doses. The highest caspases activity was observed in HepG2 cells treated with 1,000 µg/mL of nanoparticles. After 24 hours, the caspase-3 and -9 activity increased to about fivefold higher than that in the untreated cells. In comparison with untreated cells, the caspase-3 and -9 activity increased to 156% and 168% upon treatment with 100 µg/mL nanoparticles, while it increased 3.9- and 4.7-fold in MCF7 cells after treatment with 1,000 µg/mL nanoparticles. In HT29 cells, the caspase-3 activity increased significantly (2.7-fold) after treatment with 1,000 µg/mL nanoparticles. In the normal MCF10a cells, caspase-3 activity was not significantly different from that in the untreated cells at all concentrations tested.

DNA fragmentation

The relative quantity of small DNA fragments in the cells treated with 10 µg/mL nanoparticles is shown in Figure 10. In HepG2 and HT29 cells, NiZn ferrite nanoparticle treatment increased fragmented DNA in a time- and concentration-dependent manner. The increase in concentration of nanoparticles from 100 to 1,000 µg/mL did not significantly affect the relative quantity of DNA fragments in MCF7 cells after 12 hours of treatment. However, exposure to 1,000 µg/mL nanoparticles produced higher DNA fragmentation in HepG2, MCF7, and HT29 cells at 38.5% ± 3.6%, 13.4% ± 1.7%, and 11.8% ± 1.5%, respectively, than in the untreated cells at 3.6% ± 0.9%, 4.1% ± 1.1%, and 2.5% ± 0.7%, respectively.

Discussion

The role of NiZn ferrite nanoparticles in biomedical applications can be attributed to their magnetic properties, particularly under cryogenic temperatures, which verify their superparamagnetic nature. The magnetic properties of these magnetic nanoparticles have been discussed.[21]

In vitro cytotoxicity testing can be done efficiently and economically in a previous study and is used to screen
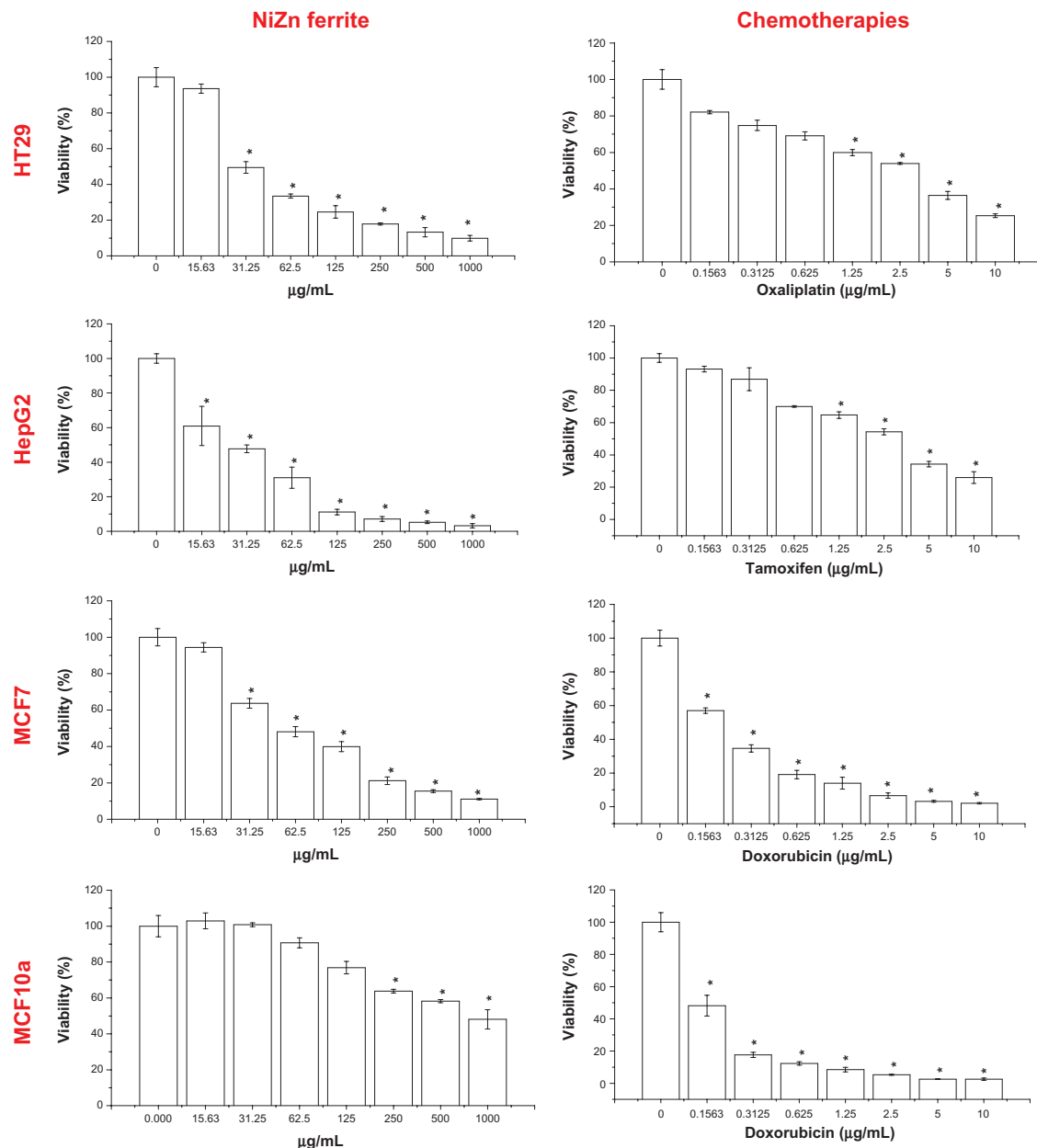
Figure 6 NiZn ferrite nanoparticles and chemotherapeutic effects on the viability of treated cells, which were evaluated through mitochondrial activity using MTT assay.
Notes: Mean ± SD (n = 3 wells/treatment); *$P < 0.05$ compared with the untreated cells.
Abbreviations: SD, standard deviation; MTT, (3-(4,5-dimethylthiazol-2-yl)-2,5-diphenyltetrazolium bromide); NiZn, nickel zinc.

Table I IC_{50} of NiZn ferrite nanoparticles, oxalipatin, doxorubicin, and tamoxifen on HT29, MCF7, HepG2, and MCF10a cells after 72 hours

Treatment	IC_{50} (µg/mL)			
	HT29	MCF7	HepG2	MCF10a
NiZn ferrite nanoparticles	31.1 ± 1.2	58.7 ± 9.1	28.5 ± 1.4	915.0 ± 2.9
Oxaliplatin	3.06 ± 0.3	–	–	–
Doxorubicin	–	0.21 ± 0.1	–	0.15 ± 0.2
Tamoxifen	–	–	3.04 ± 1.1	–

Note: Mean ± SD.
Abbreviations: IC_{50}, concentration of drug needed to inhibit cell growth by 50%; SD, standard deviation.

chemicals before testing in animal studies.[22,23] The concentration response is an important part of cytotoxicity determinations, which should be included to provide a preclinical evaluation of the range over which toxicant-induced cytotoxicity or response occurs.[24] As demonstrated in Figures 6 and 7, it is evident that HepG2, HT29, and MCF7 cells responded differently to NiZn ferrite nanoparticle exposure. The viability values indicate that HepG2 cells were more sensitive to the nanoparticles than either MCF7 or HT29 cells after 72 hours exposure while normal breast MCF10a cells exhibited the highest resis-
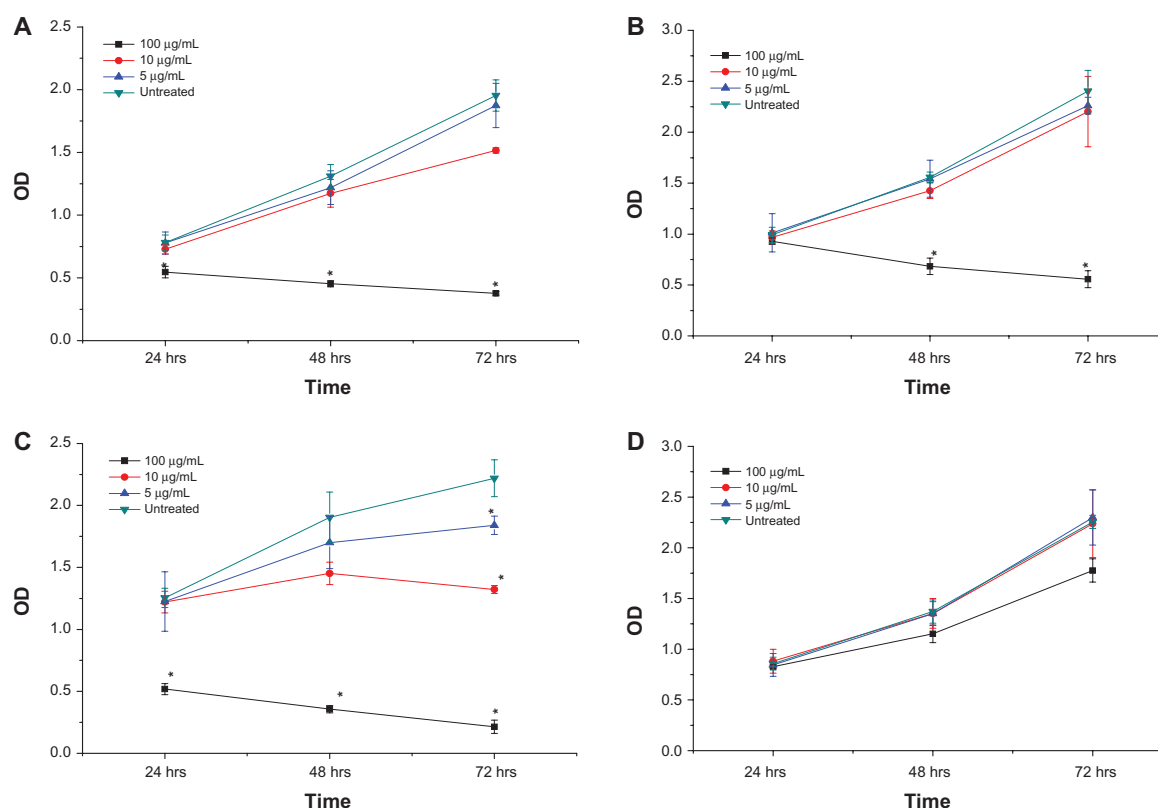
Figure 7 Effects of NiZn magnetic nanoparticles on the proliferation of (**A**) HT29, (**B**) MCF7, (**C**) HepG2, and (**D**) MCF10a cells in vitro.
Notes: The nanoparticle inhibits cell proliferation in a time- and dose-dependent manner. After treatment with different concentrations of nanoparticles for 24, 48, and 72 hours, the proliferation of the cells was determined by BrdU assay. Mean ± SD (n = 3 wells/treatment); * $P < 0.05$ compared with the untreated cells.
Abbreviations: hrs, hours; SD, standard deviation; OD, optical density.

tance. Using normal cell lines to compare the cytotoxicity effects of NiZn magnetic nanoparticles with cancer cell lines is advisable to confirm these results. This is an important consideration when evaluating a newly formulated drug.[25] Hathaway et al[26] developed a biologically targeted

magnetic nanoparticle that exploits differences between MCF7, BT-474, and MDA-MB-231 breast cancer cells and normal Chinese hamster ovary cells, which permits greater specificity for cancer cells with less damage to normal cells.
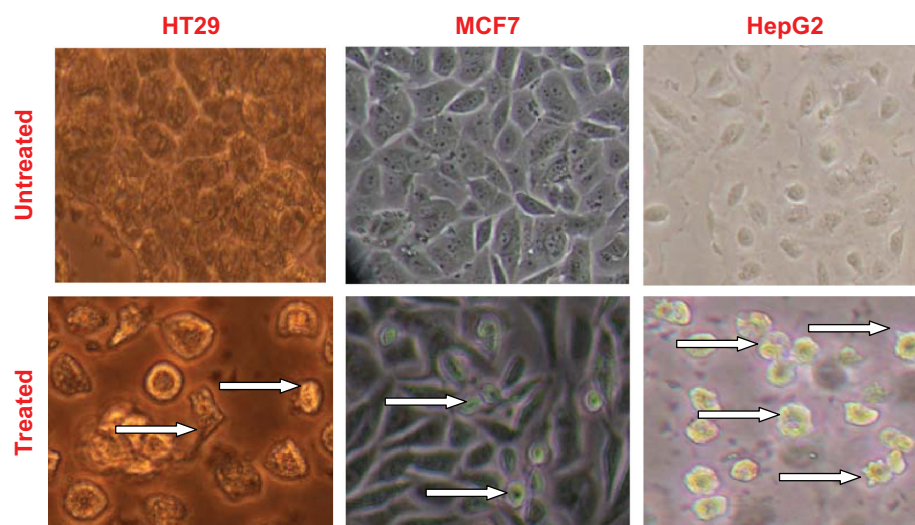

Figure 8 The morphological changes of HepG2, HT29, and MCF7 cells treated with NiZn magnetic nanoparticles at their respective IC$_{50}$ concentrations for 72 hours.
Note: White arrows indicate apoptotic cells with typical membrane blebbing (200×).
Abbreviation: IC$_{50}$, concentration of drug needed to inhibit cell growth by 50%; NiZn, nickel zinc.
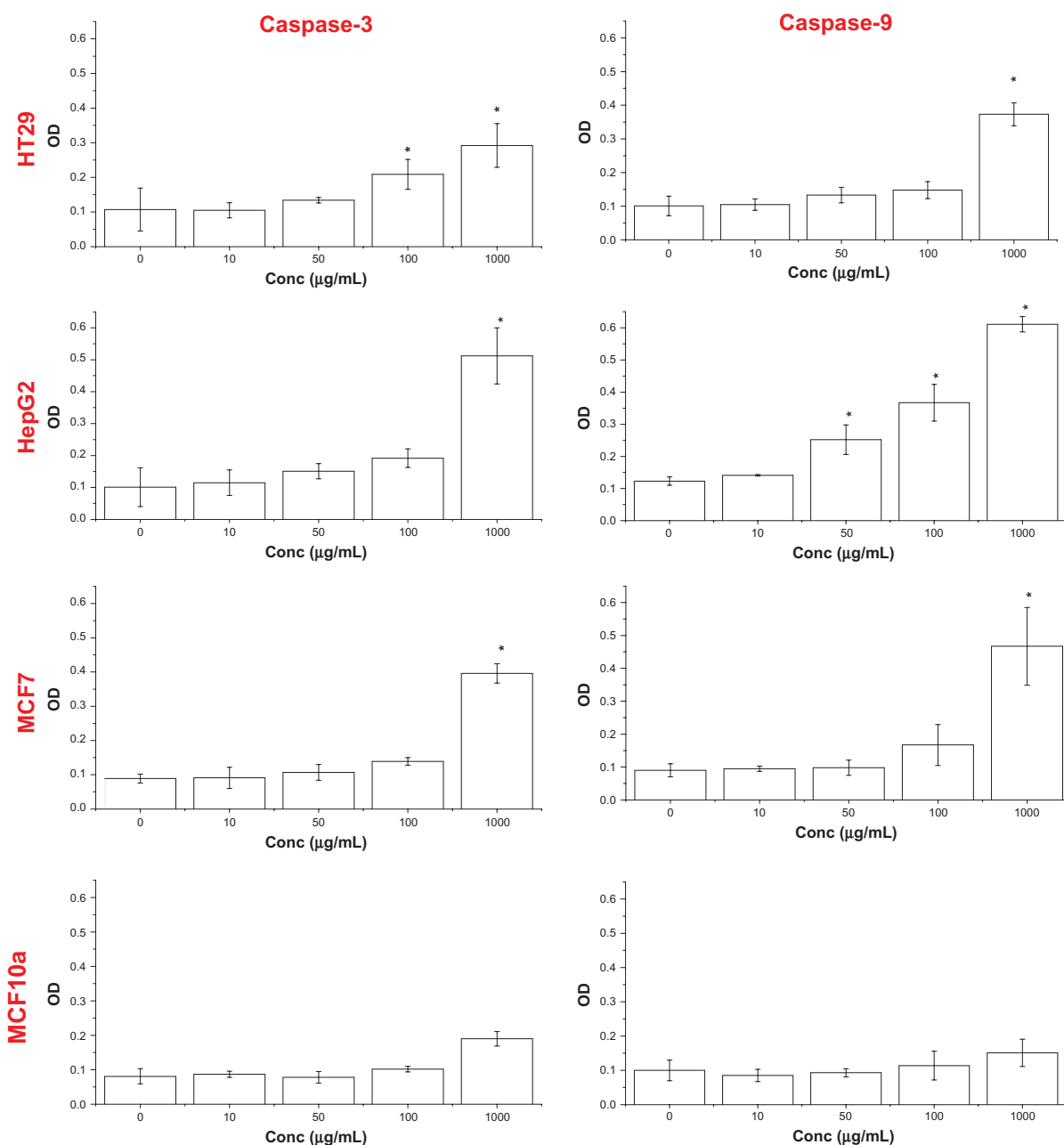
Figure 9 Treatment of HepG2, HT29, MCF10a, and MCF7 cells with NiZn magnetic nanoparticles results in activation of caspase-3 and -9.
Notes: Cells were treated with 10, 50, 100, and 1,000 µg/mL for 24 hours, and then caspase-3 and -9 activities were determined using the CaspAce® system (Promega, Madison, WI, USA). Mean ± SD (n = 3 wells/treatment). *$P < 0.05$ compared with the untreated cells.
Abbreviations: NiZn, nickel zinc; SD, standard deviation; OD, optical density.

Time-response studies are also useful in cytotoxicity determinations because they are indicators of association between functional change and irreversible cell damage.[27,28] The 72 hours of incubation with NiZn ferrite nanoparticles had the most inhibitory effects in BrdU incorporation assays, with loss of cell viability being both dose- and time-dependent. At 72 hours, HepG2 and HT29 cells retained 60% and 77% of controlled proliferation after treatment with 10 µg/mL nanoparticles, respectively, while in MCF7 cells, controlled proliferation was reduced

to 91%. The cytotoxicity of NiZn ferrite nanoparticles is similar to that of another magnetic nanoparticle ie, nickel ferrite nanoparticles, which exhibited antitumor activities in human alveolar adenocarcinoma A549 cell lines at 100 µg/mL.[19]

In another supporting study, nickel ferrite nanoparticles prepared by a different method, have shown similar effects on the cervical adenocarcinoma HeLa cell lines.[18] At 10 µg/mL, nickel ferrite nanoparticles produced only slight antitumor activity. However, the effect was more pronounced after
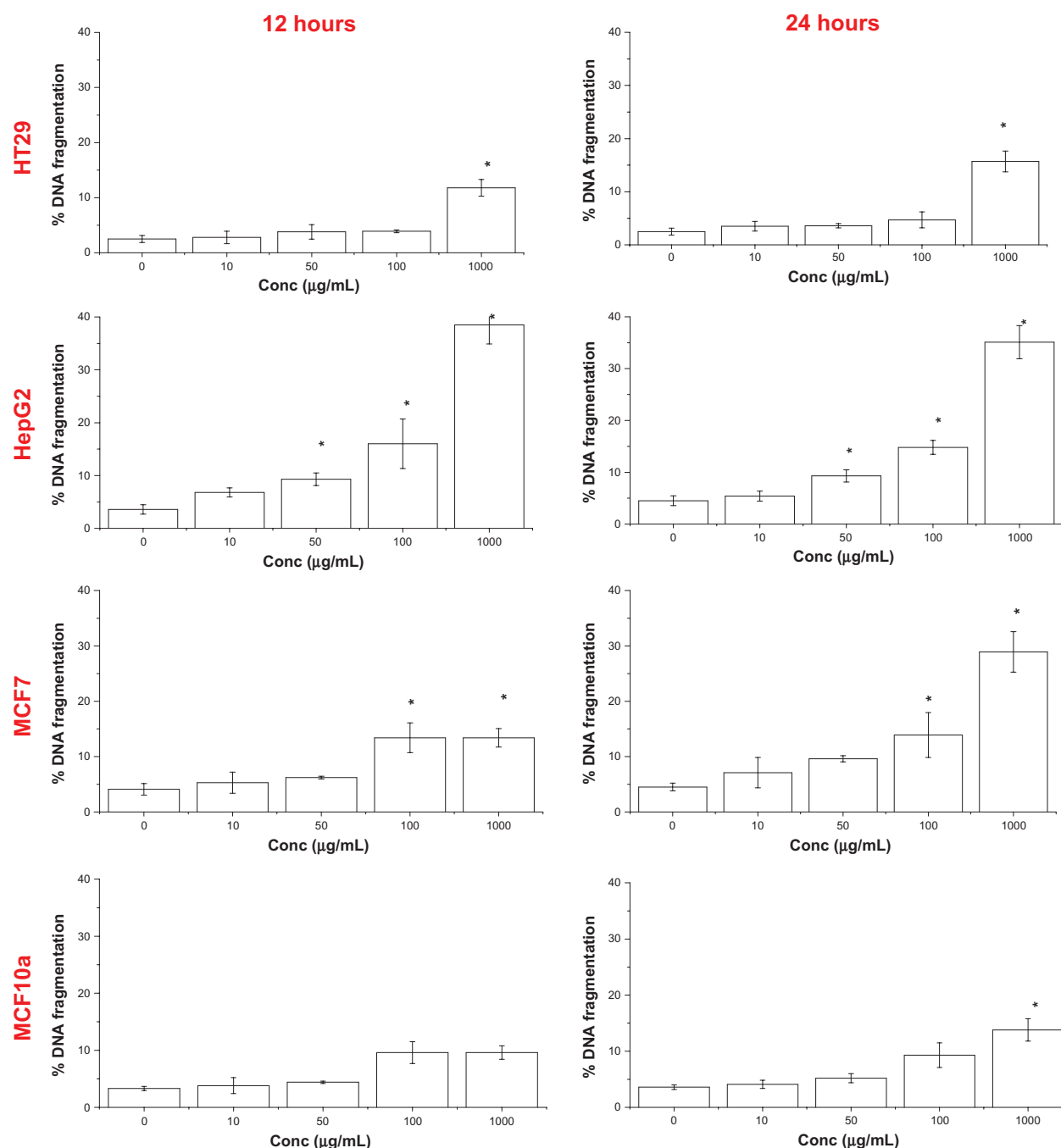
Figure 10 Quantitation of DNA fragments induced by NiZn ferrite nanoparticles.
Notes: HepG2, HT29, MCF10a, and MCF7 cells were treated with the nanoparticles for 12 and 24 hours. The amount of DNA fragments was determined by DPA and compared to that of total DNA. Mean $\pm$ SD (n = 3 wells/treatment); $*P < 0.05$ compared with the untreated cells.
Abbreviations: Conc, concentration; DNA, deoxyribo-nucleic acid; DPA, diphenylamine; NiZn, nickel zinc; SD, standard deviation.

72 hours with 83% cytotoxicity compared to untreated cells.[18] However, these results are clearly distinct from previous findings, in which 1,000 µg/mL magnetic nanoparticles showed a slight inhibition in both human umbilical vein endothelial cells and PC3 prostate cancer cells incubated for 48 hours.[29]

Cells treated with NiZn ferrite nanoparticles have been shown to manifest the characteristic morphological changes associated with apoptosis or programmed cell death. In fact, a light microscope revealed the morphological characteristics of apoptosis that are attributed to the cytotoxic effect of the nanoparticles. Magnetic nanoparticle-induced apoptosis may

be an integral component of the cellular mechanism relating to its therapeutic effects and cytotoxicities. The magnetic nanoparticles are rapidly distributed in epithelial tissue with strong binding to plasma proteins, principally albumin.[30]

Activation of endogenous nuclease enzymes is considered to be a key biochemical event in apoptosis, leading to the cleavage of DNA into nucleosomesized fragments, and it is well-known that caspase-3 is a key mediator of nuclease activation.[31] The three cell lines, HT29, MCF7, and HepG2, were treated with increasing concentrations of NiZn ferrite nanoparticles to determine conditions that could induce apoptosis as measured by a standard interchromosomal DNA fragmentation assay. NiZn ferrite nanoparticles induced dose-dependent apoptosis in the treated cells with maximal effective dose of about 100 μg/mL in HepG2 cells and 1,000 μg/mL for both HT29 and MCF7 cells after 12 hours. This effect is similar to that produced by nickel ferrite nanoparticles, but in the human alveolar adenocarcinoma A549 cell line with a similar effective concentration of 100 μg/mL or less.[19] Nevertheless, previous data has provided evidence that magnetic nanoparticles fulfill two basic criteria for an effective chemotherapeutic agent, ie, tumor specificity and minimal toxicity to normal cells.[26]

Conclusion

NiZn ferrite nanoparticles exhibited greater cytotoxicity on liver cancer HepG2 cells among the cancer cell lines examined. The normal breast MCF10a cells seemed to show the lowest sensitivity to the cytotoxic effect of the nanoparticles. NiZn ferrite nanoparticles selectively killed liver cancer cells through suppression of proliferation and induction of apoptosis. Our magnetic nanoparticles induced apoptosis in cancer cells via a caspase-9-dependent pathway. In fact, a significant increase of caspase-3 activity, which correlates with the DPA assay findings, a marker of DNA fragmentation, was observed in HT29, MCF7, and HepG2 cell lines as a result of treatment with NiZn ferrite nanoparticles.

Extrapolation of the in vitro cytotoxic effects of our NiZn ferrite nanoparticles to in vivo anticancer application would require further studies to determine its stability, half-life, and biologically significant concentrations in the induction of the apoptotic pathway in vivo. Therefore, taking this into consideration, our findings strongly suggest that NiZn ferrite nanoparticles merit further investigation as a cancer chemotherapeutic agent.

Disclosure

The authors report no conflicts of interest in this work.

References

1. Sun C, Lee JSH, Zhang M. Magnetic nanoparticles in MR imaging and drug delivery. *Adv Drug Deliv Rev*. 2008;60(11):1252–1265.
2. Gu H, Ho PL, Tsang KWT, Wang L, Xu B. Using biofunctional magnetic nanoparticles to capture vancomycin-resistant enterococci and other gram-positive bacteria at ultralow concentration. *J Am Chem Soc*. 2003;125(51):15702–15703.
3. Taylor EN, Webster TJ. The use of superparamagnetic nanoparticles for prosthetic biofilm prevention. *Int J Nanomedicine*. 2009;4:145–152.
4. Peyre J, Humblot V, Méthivier C, Berjeauc JM, Pradier CM. Co-grafting of amino-poly-ethylene-glycol and magainin I on a TiO₂ surface: Tests of antifouling and antibacterial activities. *J Phys Chem B*. 2012;116(47):13839–13847.
5. Lee KJ, An JH, Shin JS, Kim DH. Synthesis and characterization of bicalutamide-loaded magnetic nanoparticles as anti-tumor drug carriers. *J Nanosci Nanotechnol*. 2012;12(2):1611–1615.
6. Kircher MF, Mahmood U, King RS, Weissleder R, Josephson L. A multimodal nanoparticle for preoperative magnetic resonance imaging and intraoperative optical brain tumor delineation. *Cancer Res*. 2003;63(23):8122–8125.
7. Brunke O, Odenbach S, Jurgons R, Alexiou C, Hilger I, Beckmann F. Determination of the magnetic particle distribution in tumour tissue by means of x-ray tomography. *J Phys Condens Matter*. 2006;18(38):S2903.
8. Pray L. *Molecular Diagnostics: New Growth, New Markets*. Waltham, MA: Cambridge Healthtech Advisors; 2005.
9. Leuschner C, Kumar CSSR, Hansel W, Soboyejo W, Zhou J, Hormes J. LHRH-conjugated magnetic iron oxide nanoparticles for detection of breast cancer metastases. *Breast Cancer Res Treat*. 2006;99(2):163–176.
10. Zhao Q, Wang L, Cheng R, et al. Magnetic nanoparticle-based hyperthermia for head and neck cancer in mouse models. *Theranostics*. 2012;2(1):113–121.
11. Thomas LA, Dekker L, Kallumadil M, et al. Carboxylic acid-stabilised iron oxide nanoparticles for use in magnetic hyperthermia. *J Mater Chem*. 2009;19(36):6529–6535.
12. Babincov M, Altanerov V, Altaner C, Bergemann C, Babinec P. In vitro analysis of cisplatin functionalized magnetic nanoparticles in combined cancer chemotherapy and electromagnetic hyperthermia. *IEEE Trans Nanobiosci*. 2008;7(1):15–19.
13. Maeng JH, Lee DH, Jung KH, et al. Multifunctional doxorubicin-loaded superparamagnetic iron oxide nanoparticles for chemotherapy and magnetic resonance imaging in liver cancer. *Biomaterials*. 2010;31(18):4995–5006.
14. Jia Y, Yuan M, Yuan H, et al. Co-encapsulation of magnetic Fe3O4 nanoparticles and doxorubicin into biodegradable PLGA nanocarriers for intratumoral drug delivery. *Int J Nanomedicine*. 2012;63:1697–1708.
15. Martin J. *British National Formulary: September 2010*. London. BMJ Group and RPS Publishing; 2010.
16. de Freitas ERL, Soares PRO, de Paula Santos R, et al. In vitro biological activities of anionic-Fe₂O₃ nanoparticles on human melanoma cells. *J Nanosci Nanotechnol*. 2008;8(5):2385–2391.
17. Yang G, Li X, Zhao Z, Wang W. Preparation, characterization, in vivo and in vitro studies of arsenic trioxide Mg-Fe ferrite magnetic nanoparticles. *Acta Pharmacol Sin*. 2009;30(12):1688–1693.
18. Tomitaka A, Koshi T, Hatsugai S, Yamada T, Takemura Y. Magnetic characterization of surface-coated magnetic nanoparticles for biomedical application. *J Magn Magn Mater*. 2011;323(10):1398–1403.
19. Ahamed M, Akhtar MJ, Siddiqui MA, et al. Oxidative stress mediated apoptosis induced by nickel ferrite nanoparticles in cultured A549 cells. *Toxicology*. 2011;283(2–3):101–108.

20. Modak S, Ammar M, Mazaleyrat F, Das S, Chakrabarti PK. XRD, HRTEM and magnetic properties of mixed spinel nanocrystalline Ni−Zn−Cu−ferrite. *J Alloys Compd*. 2009;473(1–2):15–19.

21. Flaifel MH, Ahmad SH, Abdullah MH, Al-Asbahi BA. NiZn Ferrite filled thermoplastic natural rubber nanocomposites: effect of low temperature on their magnetic behaviour. *Cryogenics*. 2012;52(10):523–529.

22. Malich G, Markovic B, Winder C. The sensitivity and specificity of the MTS tetrazolium assay for detecting the in vitro cytotoxicity of 20 chemicals using human cell lines. *Toxicology*. 1997;124(3):179–192.

23. Shokri F, Heidari M, Gharagozloo S, Ghazi-Khansari M. In vitro inhibitory effects of antioxidants on cytotoxicity of T-2 toxin. *Toxicology*. 2000;146(2):171–176.

24. Miller FJ, Schlosser PM, Janszen DB. Haber's rule: a special case in a family of curves relating concentration and duration of exposure to a fixed level of response for a given endpoint. *Toxicology*. 2000;149(1): 21–34.

25. Al-Qubaisi M, Rozita R, Yeap SK, Omar AR, Ali AM, Alitheen NB. Selective cytotoxicity of goniothalamin against hepatoblastoma HepG2 cells. *Molecules*. 2011;16(4):2944–2959.

26. Hathaway HJ, Butler KS, Adolphi NL, et al. Detection of breast cancer cells using targeted magnetic nanoparticles and ultra-sensitive magnetic field sensors. *Breast Cancer Res*. 2011;13(5):R108.

27. Rozman KK, Doull J. Dose and time as variables of toxicity. *Toxicology*. 2000;144(1):169–178.

28. Tennekes HA. The significance of the Druckrey–Küpfmüller equation for risk assessment – The toxicity of neonicotinoid insecticides to arthropods is reinforced by exposure time: Responding to a Letter to the Editor by Drs C Maus and R Nauen of Bayer CropScience AG. *Toxicology*. 2011;280(3):173.

29. Häfeli UO, Riffle JS, Harris-Shekhawat L, et al. Cell uptake and in vitro toxicity of magnetic nanoparticles suitable for drug delivery. *Mol Pharm*. 2009;6(5):1417–1428.

30. Lartigue L, Wilhelm C, Servais J, et al. Nanomagnetic sensing of blood plasma protein interactions with iron oxide nanoparticles: impact on macrophage uptake. *ACS Nano*. 2012;6(3):2665–2678.

31. Mitamura S, Ikawa H, Mizuno N, Kaziro Y, Itoh H. Cytosolic nuclease activated by caspase-3 and inhibited by DFF-45. *Biochem Biophys Res Comm*. 1998;243(2):480–484.